Pharmaceutical Research, Vol. 23, No. 12, December 2006 (© 2006)
DOI: 10.1007/s11095-006-9122-2

Research Paper

Transport of Poly(Amidoamine) Dendrimers across Caco-2 Cell Monolayers: Influence of Size, Charge and Fluorescent Labeling

Kelly M. Kitchens,[1] Rohit B. Kolhatkar,[1] Peter W. Swaan,[1] Natalie D. Eddington,[1] and Hamidreza Ghandehari [1,2,3]

Received February 6, 2006; accepted July 14, 2006; published online November 9, 2006

Purpose. To investigate the transport of poly(amidoamine) (PAMAM) dendrimers with positive, neutral and negatively charged surface groups across Caco-2 cell monolayers.
Methods. Cationic PAMAM-NH_2 (G2 and G4), neutral PAMAM-OH (G2), and anionic PAMAM-COOH (G1.5–G3.5) dendrimers were conjugated to fluorescein isothiocyanate (FITC). The permeability of fluorescently labeled PAMAM dendrimers was measured in the apical-to-basolateral direction. ^{14}C-Mannitol permeability was measured in the presence of unlabeled and FITC labeled PAMAM dendrimers. Caco-2 cells were incubated with the dendrimers followed by mouse anti-occludin or rhodamine phalloidin, and visualized using confocal laser scanning microscopy to examine tight junction integrity.
Results. The overall rank order of PAMAM permeability was G3.5COOH > G2NH_2 > G2.5COOH > G1.5COOH > G2OH. ^{14}C-Mannitol permeability significantly increased in the presence of cationic and anionic PAMAM dendrimers with significantly greater permeability in the presence of labeled dendrimers compared to unlabeled. PAMAM dendrimers had a significant influence on tight junction proteins occludin and actin, which was microscopically evidenced by disruption in the occludin and rhodamine phalloidin staining patterns.
Conclusions. These studies demonstrate that enhanced PAMAM permeability is in part due to opening of tight junctions, and that by appropriate engineering of PAMAM surface chemistry it is possible to increase polymer transepithelial transport for oral drug delivery applications.

KEY WORDS: Caco-2 cells; oral drug delivery; poly(amidoamine) dendrimers; tight junctions; transport.

INTRODUCTION

The central component of many controlled drug delivery systems is a polymeric biomaterial. Polymers exhibit low permeability across epithelial barriers due to their large size. Therefore, a major limitation of polymers in oral drug delivery systems is their limited transport across epithelial barriers. For instance, the tight junctions of the intestinal epithelium have a pore size of approximately 10–30 Å (1), whereas the hydrodynamic volumes of conventional water-soluble polymers range from few to several hundred nanometers (2,3). Due to their large size, polymer-drug conjugates are usually administered parenterally to directly deliver the drug to the systemic circulation and bypass the gastrointestinal system. However, it is highly desirable to develop new polymeric drug delivery systems that are orally bioavailable and would lead to high patient compliance. One class of polymeric carriers that has shown potential in oral drug delivery is the poly(amidoamine) (PAMAM) dendrimer family (4–11). Dendrimers are macromolecules with defined mass, size, shape, topology and surface chemistry (12,13). Starburst dendrimers are characterized by a unique tree-like branching architecture that starts from an initiator core around which the branches of the dendrimer originate. Each branching series is termed as a generation (G). Dendrimers with terminal amine groups are termed as "full generation" and are symbolized with a full number (e.g., G1, G2, etc.), and termed as "half generation" with terminal carboxylate groups (e.g., G0.5, G1.5, etc.). PAMAM dendrimers have potential use in drug delivery due to the high degree of branching, which allows the polymer-drug conjugate to have a high density of biological agents in a compact system.

Recent studies have demonstrated that surface chemistry influences the transport of PAMAM dendrimers across the epithelial barrier of the gut (5,7,8). Initial studies suggest that both positively (7) and negatively (5,8) charged dendrimers

[1] Center for Nanomedicine and Cellular Delivery, Department of Pharmaceutical Sciences, University of Maryland, Baltimore, Baltimore, Maryland, USA.
[2] Department of Pharmaceutical Sciences, University of Maryland School of Pharmacy, 20 Penn Street, HSFII Room 625, Baltimore, Maryland 21201-1075, USA.
[3] To whom correspondence should be addressed. (e-mail: hghandeh@rx.umaryland.edu)

ABBREVIATIONS: FITC, Fluorescein isothiocyanate; G, Generation; HBSS, Hank's balanced salt solution; PAMAM, Poly(amidoamine); TEER, Transepithelial electrical resistance.

permeate across epithelial barriers to an appreciable extent relative to their size and result in increased ^{14}C-mannitol transport (7,8). PAMAM-NH_2 dendrimers decreased transepithelial electrical resistance (TEER) readings and increased ^{14}C-mannitol permeability with an increase in generation number and dendrimer size; PAMAM-OH dendrimers did not influence TEER or ^{14}C-mannitol transport; and, PAMAM-COOH dendrimers decreased TEER and increased ^{14}C-mannitol permeability within a specific size window (G2.5 and G3.5) (7,8). These studies point to a size and charge window of PAMAM dendrimers that can effectively translocate drug molecules across the epithelial barrier of the gut. However, a systematic correlation between the effect of size, charge and extent of surface modification of these polymers on their permeability across the intestinal barrier has not been evaluated.

Previous studies in our laboratory (7) investigated the permeability of a series of PAMAM-NH_2 dendrimers (generations 0–4), in which results demonstrated a generation-dependent permeability profile. In the present work we assessed the affect of dendrimer size and charge by studying the permeability of cationic PAMAM-NH_2 (G2), neutral PAMAM-OH (G2), and anionic PAMAM-COOH (G1.5–G3.5) labeled with fluorescein isothiocyanate (FITC). $G2NH_2$ was selected among the cationic dendrimers since this dendrimer had appreciable permeability relative to its molecular size and was non-toxic to Caco-2 cell monolayers. To systematically compare the effect of surface charge, the permeability of a well-characterized paracellular transport marker, ^{14}C-mannitol, was used as an internal standard in the presence of structurally related dendrimers that are similar to $G2NH_2$ and vary in surface charge (i.e., G2OH and G1.5COOH). Since $G4NH_2$ dendrimers were previously reported to be toxic to Caco-2 cells (7), our aim was to investigate how surface modification with FITC molecules would affect $G4NH_2$ toxicity as well as permeability. Confocal laser scanning microscopy was used to visualize the effect of PAMAM dendrimers on cellular tight junctions. The results from this research will aid in understanding the relationship between dendrimer structural properties and their transepithelial transport, which is useful in selecting suitable dendrimers for use in orally active polymeric drug delivery systems.

MATERIALS AND METHODS

Materials

PAMAM dendrimer solutions ($G2NH_2$, $G4NH_2$, G2OH, G1.5–G3.5COOH), fluorescein isothiocyanate, ^{14}C-mannitol (specific activity 50 mCi/mmole) and Triton X-100 were purchased from Sigma-Aldrich Co. (St. Louis, MO). Superose 12 HR 16/50 column and Superose 12 preparative grade beads were purchased from Amersham Pharmacia Biotech (Piscataway, NJ). Caco-2 cells were purchased from American Type Cell Culture (ATCC, Rockville, MD). Mouse anti-occludin, Alexa Fluor 488 goat anti-mouse IgG, and rhodamine phalloidin were purchased from Invitrogen Co. (Carlsbad, CA). WST-1 cell proliferation reagent was purchased from Roche Applied Science (Indianapolis, IN).

Fluorescent Labeling of PAMAM Dendrimers

Cationic (G2) and anionic (G1.5–G3.5) PAMAM dendrimers were reacted with FITC at a feed molar ratio of 1:1, in which the anionic dendrimers were first modified with ethylenediamine (5). Aqueous solutions of anionic PAMAM dendrimers were mixed with aqueous solutions of *N*-(3-dimethylaminopropyl)-*N′*-ethylcarbodiimide (EDC) at a molar ratio of 1:1 for 30 min at room temperature. A molar equivalent of ethylenediamine was added to the reaction, which was then incubated for 4 h at room temperature. Cationic and anionic PAMAM dendrimers were conjugated to FITC as follows. PAMAM dendrimers were dissolved in phosphate buffered saline (PBS) at pH 7.4. The corresponding amount of FITC was dissolved in acetone (<5 mg/ml), added to the PAMAM solutions and allowed to stir overnight at room temperature. Neutral (G2) PAMAM dendrimers were dissolved in dimethyl formamide (DMF). The corresponding amounts of FITC and triethylamine (TEA) (molar ratio of PAMAM:FITC:TEA = 1:1:1) were dissolved in DMF, added to PAMAM solutions and allowed to stir for 72 h in nitrogen atmosphere at 80°C. Generation 4 cationic dendrimers ($G4NH_2$) were dissolved in dimethyl sulfoxide (DMSO). FITC was dissolved in DMSO, then conjugated to $G4NH_2$ overnight in nitrogen atmosphere at room temperature with feed molar ratios of 1:1, 1:4 and 1:8 ($G4NH_2$:FITC).

Fluorescently labeled PAMAM dendrimers were purified and fractionated following a previously reported method (14). Briefly, fluorescently labeled dendrimers were dialyzed against distilled water using dialysis membranes of 500 MWCO (Spectrum Laboratories, Inc., Rancho Dominguez, CA), fractionated on a Superose 12 HR 16/50 preparative column using a Fast Protein Liquid Chromatography (FPLC) system (Amersham Pharmacia Biotech, Uppsala, Sweden) using a mobile phase of 30%/70% (v/v) acetonitrile:Tris buffer (pH 8.0) and a flow rate of 1.0 ml/min. Eluting molecules were detected using a UV detector at 280 nm. Fractions corresponding to the appropriate dendrimer size and molecular weight were collected, dialyzed against distilled water, lyophilized and stored at 4°C for permeability and uptake experiments. The extent of FITC labeling was measured using an Ultrospec 4000 UV–vis spectrophotometer (Biochrom Ltd., Cambridge, UK) at wavelength 495 nm, and correlating the absorbance with a FITC calibration curve. The percent of substituted surface groups corresponds to the number of FITC molecules incorporated per number of dendrimer surface groups.

Caco-2 Cell Culture

Caco-2 cells (passages 30–60) were grown at 37°C in an atmosphere of 5% CO_2 and 95% relative humidity. Cells were maintained in T-75 flasks using Dulbecco's Modified Eagle's Medium (DMEM) supplemented with 10% fetal bovine serum, 1% non-essential amino acids, 10,000 units/ml penicillin, 10,000 μg/ml streptomycin and 25 μg/ml amphotericin. Growth medium was changed every 2 days. Cells were passaged at 70–90% confluency using 0.25% trypsin/ethylenediamine tetraacetic acid (EDTA) solution. Transport medium consisted of Hank's balanced salt solution (HBSS) supplemented with 10 mM *N*-(2-hydroxyethyl)piperazine-*N′*-

(2-ethanesulfonic acid) hemisodium salt (HEPES) buffer (pH 7.4).

Cytotoxicity of PAMAM Dendrimers

Caco-2 cells were seeded at a seeding density of 30,000 cells/well in 96-well cell culture plates (Corning, Inc., Corning, NY) and maintained for 48 h under cell culture conditions described in the previous section. The cells were washed twice with HBSS transport medium, then incubated with 100 μl PAMAM dendrimer and FITC samples. After 2 h, the cells were washed three times with HBSS to remove the dendrimers and replaced with 100 μl HBSS. Thereafter, 10 μl of cell proliferation reagent WST-1 was added to each well, followed by an incubation period of 4 h. Absorbance was measured at 440 nm using a SpectraMax 384 Plus plate reader (Molecular Devices, Sunnyvale, CA). Student's *t*-test ($P < 0.05$) was used to identify significant differences between PAMAM dendrimers and the negative control, blank HBSS (SPSS® for Windows).

PAMAM Permeability Across Caco-2 Cell Monolayers

Caco-2 cells were seeded at 80,000 cells/cm^2 onto polycarbonate 12-well Transwell® filters of 3.0 μm mean pore size, 1.0 cm^2 surface area (Corning Incorporated, Corning, NY). Caco-2 cells were maintained under incubation conditions described above and used for transport experiments 21–28 days post-seeding. The transport of fluorescently labeled PAMAM dendrimers was investigated in triplicate in the apical-to-basolateral (A–B) direction at a donor concentration of 1.0 mM. Permeability experiments were conducted in a humidified atmosphere of 37°C while maintaining sink conditions by transferring the filters to a new row of wells containing 1.5 ml fresh transport medium at each time point. Samples were collected from the receiver chamber at 60 and 120 min. The cell monolayer integrity was monitored using an epithelial voltohmmeter (EVOM™) (World Precision Instruments, Inc., Sarasota, FL) to measure the TEER at $t = 0$, 60, and 120 min. At the end of the experiments, the cells were washed three times with ice-cold PBS (pH 7.4) and replaced with growth medium. The TEER was measured 6, 12, 18, 24, and 48 h after the experiment.

Permeability samples were analyzed using a high-pressure liquid chromatography (HPLC) system with fluorescence detection (Waters Corporation, Milford, MA). PAMAM samples were analyzed using a Waters C-18 5 μm column with a guard column (Phenomenex, Torrence, CA), a mobile phase of 30%/70% (v/v) acetonitrile:phosphate buffer (pH 7.4), and an isocratic flow rate of 1.0 ml/min. Fluorescently labeled PAMAM samples were detected with an excitation wavelength of 495 nm and an emission wavelength of 518 nm. The apparent permeability (P_{app}) coefficients were calculated as follows:

$$P_{app} = \frac{\partial Q}{A \cdot C_0 \cdot \partial t} \quad (1)$$

Where $\partial Q/\partial t$ is the permeability rate, A is the surface area of the membrane filter, and C_0 is the initial concentration in the donor chamber (15). Multivariate ANOVA using Tukey HSD post-hoc analysis ($P < 0.05$) was used to statistically compare the mean permeability coefficients of PAMAM permeability generated by the transport experiments (SPSS® for Windows).

^{14}C-Mannitol Permeability in the Presence of PAMAM Dendrimers

The permeability of ^{14}C-mannitol (3.3 μM) across Caco-2 cell monolayers was investigated in the presence of unlabeled and fluorescently labeled PAMAM dendrimers of different charge and similar size ($G2NH_2$, G2OH, G1.5COOH). ^{14}C-Mannitol permeability was measured in triplicate in the A–B direction in a humidified atmosphere of 37°C while maintaining sink conditions. Control experiments were conducted with ^{14}C-mannitol in the absence of PAMAM dendrimers. Samples were collected at 60 and 120 min. Cell monolayer integrity was monitored as described above. Samples were analyzed by liquid scintillation counting (Beckman Coulter, Fullerton, CA). The P_{app} of ^{14}C-mannitol was calculated, and multivariate ANOVA using Dunnett's and Tukey HSD post-hoc analysis ($P < 0.05$) was used to statistically compare the mean permeability coefficients of ^{14}C-mannitol in the presence of PAMAM.

Visualization of Tight Junctions

Caco-2 cells were seeded at 30,000 cells/cm^2 onto collagen-coated 4-chamber culture slides (BD Biosciences, Bedford, MA). Caco-2 cells were maintained under normal incubation conditions and used for transport experiments 4–7 days post-seeding. Growth medium was replaced with HBSS transport medium, and cells were equilibrated with HBSS 2 h before uptake experiments. Cells were treated with 300 μl of 1.0 mM unlabeled PAMAM solutions for 2 h. The PAMAM dendrimers were removed by washing the cells three times with PBS. The cells were fixed with 300 μl of 4% paraformaldehyde for 20 min at room temperature. Then cells were permeabilized using 0.2% Triton X-100 in blocking solution, made of 1% (w/v) bovine serum albumin (BSA) in PBS, for 20 min. Staining for tight unctional proteins are described below (16):

Occludin Visualization

The cells were washed three times with PBS then incubated with 300 μl of 1% BSA for 30 min. The blocking solution was removed and cells were incubated with 300 μl of anti-occludin at 4°C overnight. After removing anti-occludin, the cells were treated with 1% BSA as before. The blocking solution was removed, then cells were incubated with 300 μl Alexa Fluor 488 goat anti-mouse IgG for 1 h at room temperature. The cells were washed with PBS, and the chambers were removed. Gel/Mount was added to each region and slides were covered with a glass coverslip, sealed, and dried overnight at 4°C. Images were obtained using a Nikon Eclipse TE2000 inverted confocal laser scanning microscope (Nikon Instruments, Inc., Melville, NY), equipped with an argon laser. Alexa Fluor 488 was visualized with excitation and emission wavelengths of 488 and 515 nm, respectively. The 3-D confocal images were acquired using the following settings of the Nikon EZ-C1 acquisition

Table I. Structural Features of Studied PAMAM Dendrimers

Generation	Surface Group	No. Surface Groups	M_W (Da)[a]	mmol FITC/g dendrimer[b]	% Substituted
G2	$-NH_2$	16	3,256	0.3896 ± 0.0288	7.9%
G2	–OH	16	3,272	0.0604 ± 0.0001	1.3%
G1.5	–COOH	16	2,935	0.0447 ± 0.0008	0.8%
G2.5	–COOH	32	6,267	0.0016 ± 0.0001	0.3%
G3.5	–COOH	64	12,931	0.0044 ± 0.0003	0.1%
G4(1:1)	$-NH_2$	64	14,215	0.0520 ± 0.0004	1.2%
G4(1:4)	$-NH_2$	64	14,215	0.2179 ± 0.0020	4.8%
G4(1:8)	$-NH_2$	64	14,215	0.4148 ± 0.0090	9.2%

[a] Reported by the manufacturer, Dendritech, Inc., Midland, MI.[b]Label content is reported as mean ± standard deviation ($n = 3$). The percent of substituted surface groups corresponds to the number of FITC molecules incorporated per number of surface groups.

software (version 2.3, Image systems, Inc., Columbia, MD): 60× oil objective with numerical aperture = 1.4; 100 μm pinhole size; 9.64 μs scan dwell; 512 × 512 pixel size; 0.40 μm *z*-step size. Confocal images were processed using Volocity 3.6 3D imaging software (Improvision, Inc., Lexington, MA) by applying iterative deconvolution using a calculated point spread function for each channel. The mean percent increase of fluorescent signal in treated cells compared to control cells was determined using the "measure objects" tool that determines the voxel (3-dimensional pixel) count of different regions of treatment ($n = 3$). Student's *t*-test ($P < 0.05$) was used to identify significant differences between cells treated with PAMAM dendrimers and control cells.

Actin Visualization

The cells were washed twice with PBS then incubated with 300 μl of 1% BSA for 30 min. The blocking solution was removed and cells were incubated with 200 μl rhodamine phalloidin solution for 20 min at room temperature. After removal of rhodamine phalloidin, the cells were treated with 1% BSA as before. The cells were washed with PBS, and the chambers were removed. Gel/Mount was added to each region and slides were covered with a glass coverslip, sealed, and dried overnight at 4°C. Images were obtained as described above, using excitation and emission wavelengths of 543 and 605 nm, respectively, for rhodamine phalloidin.

RESULTS

Permeability of Fluorescently Labeled PAMAM Dendrimers Across Caco-2 Cells

PAMAM dendrimers of different surface charge and size ($G2NH_2$, G2OH, G1.5–G3.5COOH) were conjugated to FITC (Table I). Fluorescently labeled dendrimers were fractionated based on size exclusion chromatography principles to remove small molecular weight impurities from the conjugates. That is, large molecular weight fractions (PAMAM-FITC conjugates) eluted earlier from the column and were collected, while small molecular weight compounds (unreacted FITC) eluted later. The influence of unlabeled and FITC labeled PAMAM dendrimers on the viability of Caco-2 cells was investigated by the WST-1 cytotoxicity assay (Table II). $G2NH_2$ significantly reduced the viability ($P < 0.05$) of Caco-2 cells compared to untreated cells in HBSS at donor concentration of 1.0 mM, whereas $G2NH_2$-FITC did not significantly reduce cell viability ($P > 0.05$) at all donor

Table II. Viability of Caco-2 Cells Measured with WST-1 Assay Reagent

Concentration	0.01 mM	0.1 mM	1.0 mM
HBSS		100.0%	
$G2NH_2$	80.3% ± 10.8%	78.0% ± 6.6%	*77.3% ± 1.9%*
$G2NH_2$-FITC	88.5 ± 7.5%	92.5 ± 4.9%	86.8 ± 5.5%
G2OH	103.7 ± 10.1%	103.6 ± 7.9%	96.7 ± 3.3%
G2OH-FITC	104.1 ± 6.5%	97.8 ± 13.8%	98.8 ± 4.2%
G1.5COOH	100.5 ± 17.1%	110.3 ± 3.4%	105.4 ± 7.4%
G1.5COOH-FITC	107.2 ± 6.8%	99.5 ± 5.8%	111.8 ± 6.6%
G2.5COOH	109.1 ± 3.1%	91.6 ± 13.5%	108.3 ± 3.7%
G2.5COOH-FITC	104.3 ± 11.2%	99.7 ± 16.5%	106.7 ± 10.0%
G3.5COOH	90.7 ± 1.5%	88.6 ± 2.6%	86.8 ± 4.9%
G3.5COOH-FITC	108.1 ± 3.1%	107.0 ± 9.4%	101.7 ± 11.7%
$G4NH_2$	*66.7 ± 28.8%*	*60.2 ± 6.2%*	*38.1 ± 7.1%*
$G4NH_2$-FITC (1:1)	*58.9 ± 4.3%*	*53.8 ± 9.8%*	*53.8 ± 10.4%*
$G4NH_2$-FITC (1:4)	85.1 ± 9.4%	*76.8 ± 13.5%*	*56.3 ± 3.8%*
$G4NH_2$-FITC (1:8)	97.7 ± 4.8%	76.5 ± 3.6%	74.3 ± 4.3%
FITC	107.3 ± 35.7%	108.5 ± 40.0%	98.1 ± 38.5%
Triton X-100		*30.4 ± 18.1%*	

Results are reported as mean percentage ± standard deviation of the negative control, HBSS ($n = 3$). Italicized cells indicate a significant reduction in cell viability compared to the negative control, HBSS, based upon a *p*-value < 0.05 using Student's *t*-test.

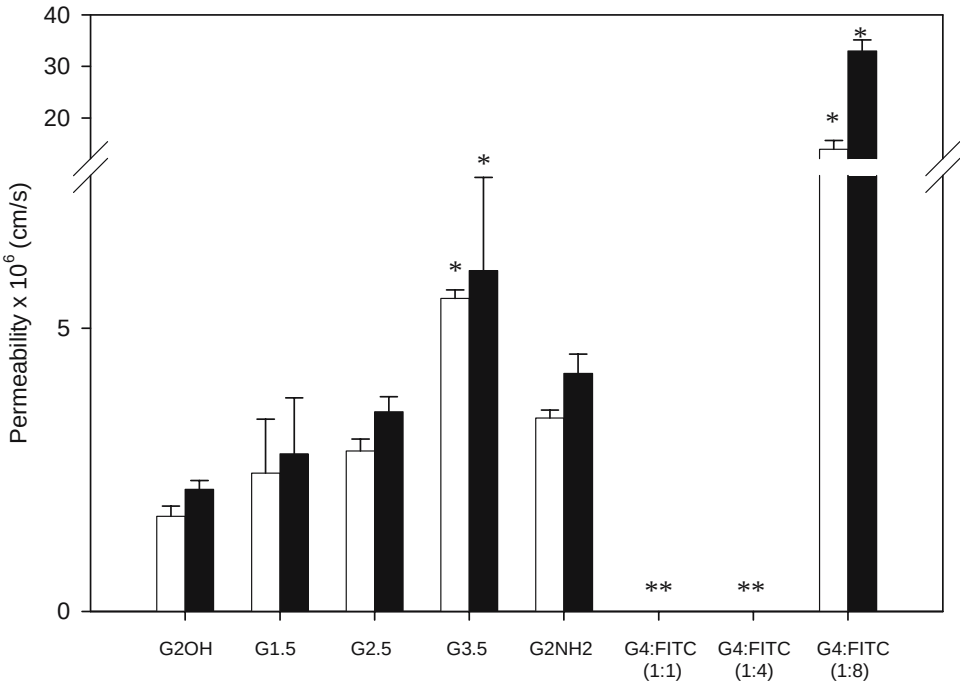

Fig. 1. The permeability of fluorescently labeled PAMAM dendrimers of donor concentration 1.0 mM across Caco-2 cell monolayers at incubation times of (□) 60 min and (■) 120 min. Permeability values are not reported (**) for dendrimers that cause toxicity. Results are reported as mean ± standard error of the mean (n = 9). (*) Denotes a significant difference in permeability compared to permeability of $G2NH_2$, G2OH, G1.5COOH, and G2.5COOH dendrimers (G3.5COOH $P < 0.05$, $G4NH_2$:FITC (1:8) $P < 0.01$).

concentrations after 2 h of dendrimer incubation. There was no significant reduction in cell viability for neutral and anionic dendrimers at donor concentrations up to 1.0 mM. The apparent permeability of PAMAM-FITC conjugates was measured in triplicate at a donor concentration of 1.0 mM up to 120 min incubation time. Permeability increased with an increase in the number of anionic surface groups in the PAMAM-COOH series (Fig. 1). The permeability of G3.5COOH was significantly greater ($P < 0.05$) than the permeability of all dendrimers studied with a 1:1 PAMAM: FITC feed molar ratio. Cationic $G2NH_2$ had greater permeability than neutral G2OH and anionic G1.5– and

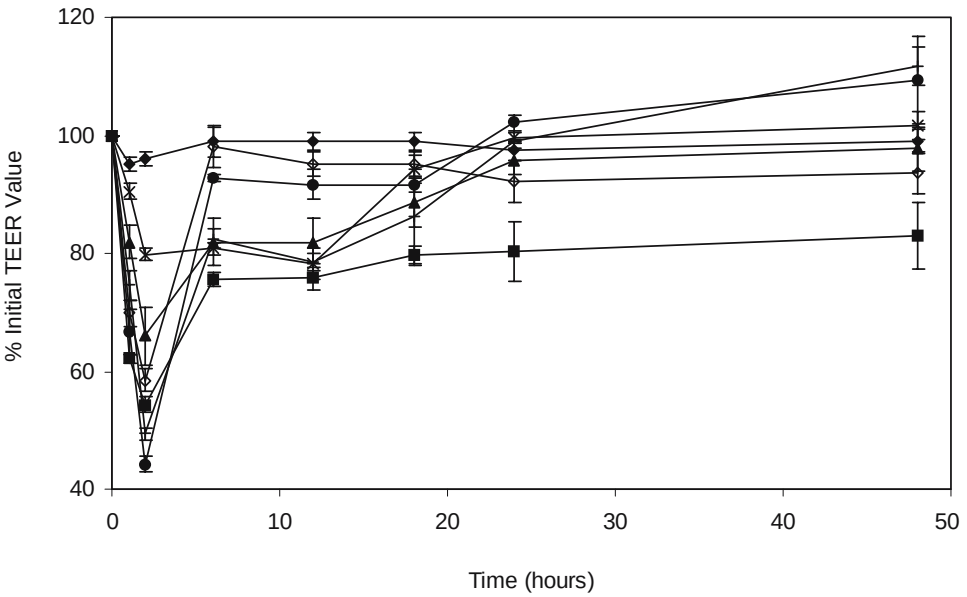

Fig. 2. Transepithelial electrical resistance of Caco-2 cells in the presence of fluorescently labeled PAMAM dendrimers as a factor of time: (♦) HBSS transport medium, (■) $G2NH_2$, (▲) G2OH, (×) G1.5COOH, (+) G2.5COOH, (●) G3.5COOH, (◊) $G4NH_2$-FITC (1:8). Results are reported as mean ± standard error of the mean (n = 9).

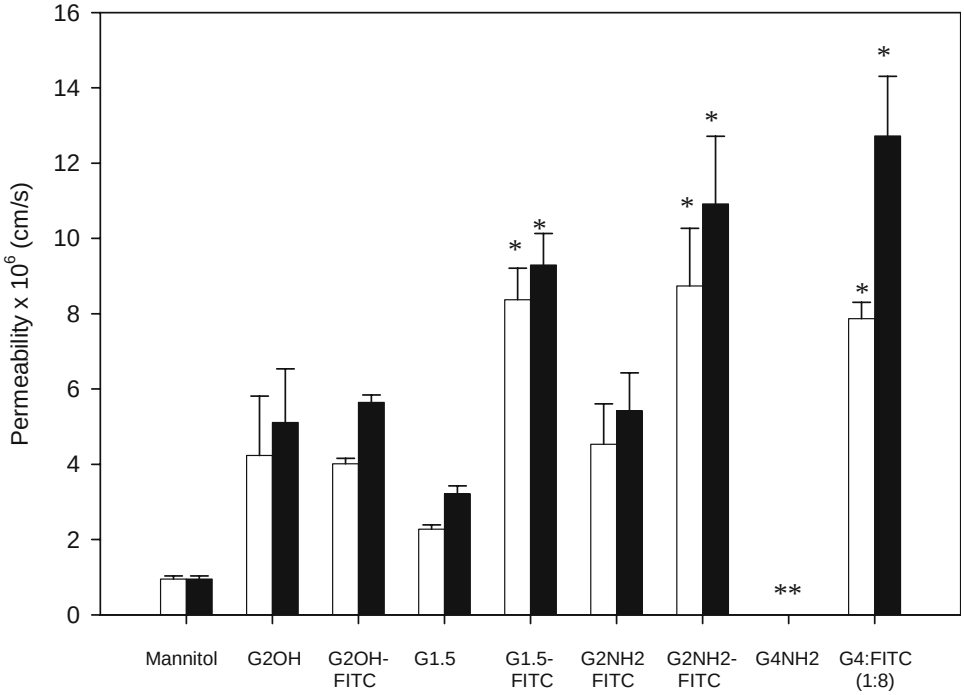

Fig. 3. The permeability of ^{14}C-mannitol (3.3 μM) in the presence of fluorescently labeled and unlabeled PAMAM dendrimers of donor concentration 1.0 mM across Caco-2 cell monolayers at incubation times of (□) 60 min and (■) 120 min. Permeability values are not reported (**) for dendrimers that cause toxicity. Results are reported as mean ± standard error of the mean (n = 9). (*) Denotes a significant increase in permeability compared to control ($P < 0.001$).

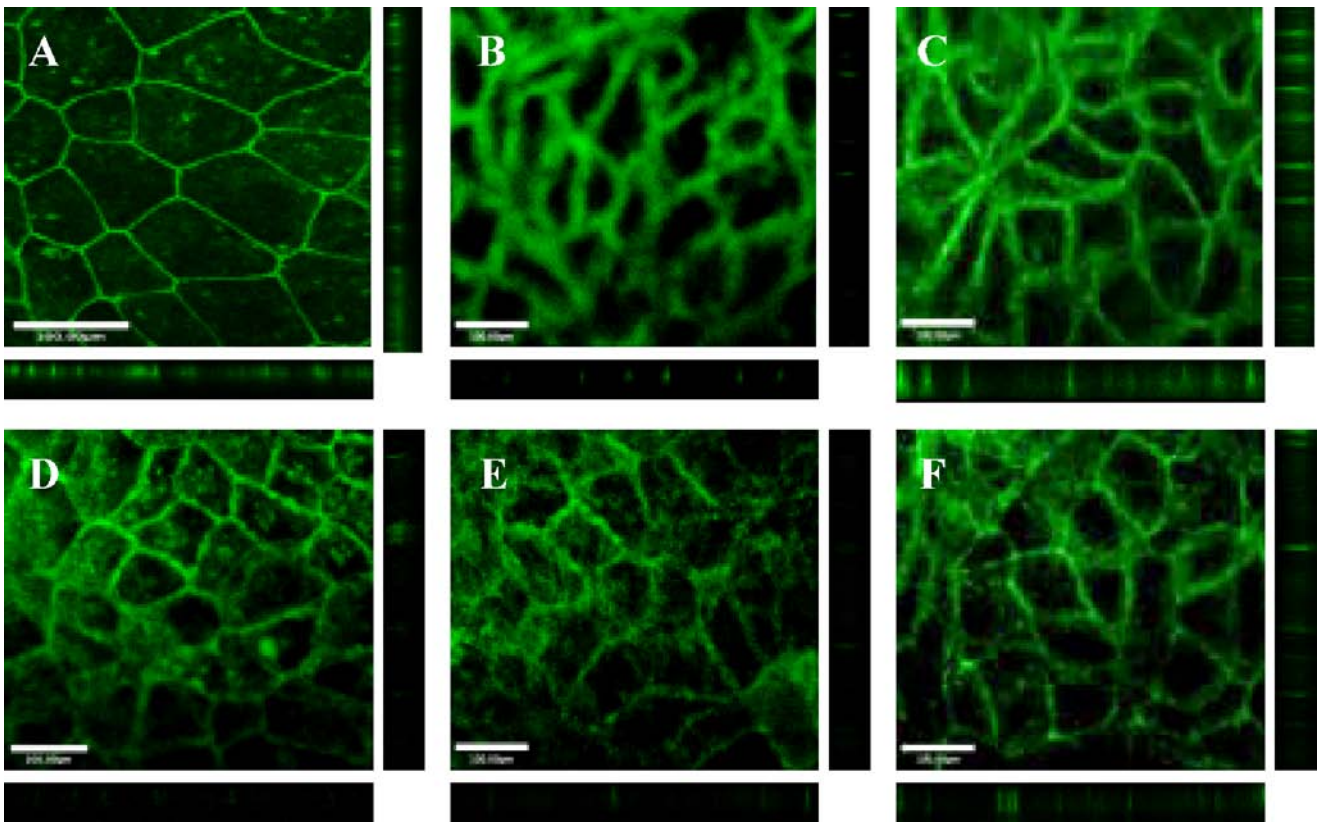

Fig. 4. Staining of the tight junction protein occludin. (A) Caco-2 cells with no polymer treatment. Caco-2 cells incubated for 120 min with 1.0 mM: (B) $G2NH_2$; (C) G2OH, (D) G1.5COOH; (E) G2.5COOH; (F) G3.5COOH. Main panels illustrate the *xy* plane; horizontal bars illustrate the *xz* plane; vertical bars illustrate the *yz* plane. Scale bars equal 100.00 μm.

G2.5COOH dendrimers (Fig. 1). The effect of all tested PAMAM dendrimers on TEER, except $G2NH_2$, was reversible after 24 h (Fig. 2).

$G4NH_2$ dendrimers were conjugated to FITC using feed molar ratios of 1:1, 1:4, and 1:8 (PAMAM:FITC). All donor concentrations of $G4NH_2$ and $G4NH_2$-FITC (1:1) significantly reduced Caco-2 cell viability ($P < 0.05$, Table II). $G4NH_2$-FITC (1:4) also significantly reduced cell viability ($P < 0.05$) at donor concentrations of 0.1 and 1.0 mM, while $G4NH_2$-FITC (1:8) did not significantly reduce cell viability ($P > 0.05$) at all donor concentrations (Table II). The permeability of $G4NH_2$-FITC (1:8) was significantly greater ($P < 0.01$) than the other dendrimers studied (Fig. 1). $G4NH_2$-FITC conjugates caused a decline in TEER up to 32% during the experiment, and only $G4NH_2$-FITC (1:8) had a reversible effect in Caco-2 cells. The TEER value of cells treated with $G4NH_2$-FITC (1:8) returned to 92.1% the original reading after 24 h (Fig. 2).

Influence of PAMAM Dendrimers on Paracellular Permeability

The permeability of ^{14}C-mannitol significantly increased in the presence of FITC labeled $G2NH_2$ ($P < 0.001$) and G1.5COOH ($P < 0.001$) dendrimers compared to their unlabeled counterparts ($P > 0.05$, Fig. 3). In a similar dendrimer size range, $G2NH_2$-FITC increased the permeability of ^{14}C-mannitol to a greater extent than G2OH-FITC and G1.5COOH-FITC. PAMAM dendrimers caused a decline in TEER over 120 min, up to 40% the original TEER values (data not shown). Decline in TEER values correlated with the increase in ^{14}C-mannitol permeability: $G2NH_2$ dendrimers caused the greatest decline in TEER, and FITC labeled dendrimers caused a greater decline in TEER than their unlabeled counterparts. Interestingly, FITC labeled PAMAM dendrimers increased ^{14}C-mannitol permeability to a greater extent than unlabeled dendrimers. To verify that ^{14}C-mannitol permeability was not increasing due to toxicity in the presence of FITC labeled dendrimers, cell viability was measured after treatment with FITC solutions using the WST-1 cytotoxicity assay. FITC did not significantly reduce cell viability ($P > 0.05$) at all donor concentrations after 2 h of incubation (Table II). The permeability of ^{14}C-mannitol in the presence of $G4NH_2$, $G4NH_2$:FITC (1:1) and $G4NH_2$:FITC (1:4) are not reported due to their toxicity. ^{14}C-mannitol permeability was highest in the presence of $G4NH_2$:FITC (1:8) at 120 min compared to other dendrimers.

PAMAM Dendrimers Cause Modulation of Tight Junctions

Cells treated with mouse anti-occludin to visualize the occludin protein displayed a uniform staining pattern encircling the cell boundary in control cells (cells not treated with PAMAM dendrimers) (Fig. 4A). Cells pretreated with PAMAM dendrimers displayed disruption in the occludin staining pattern (Fig. 4B–F). An increase in accessibility of mouse anti-occludin was evidenced in cells treated with all PAMAM dendrimers, especially for charged dendrimers.

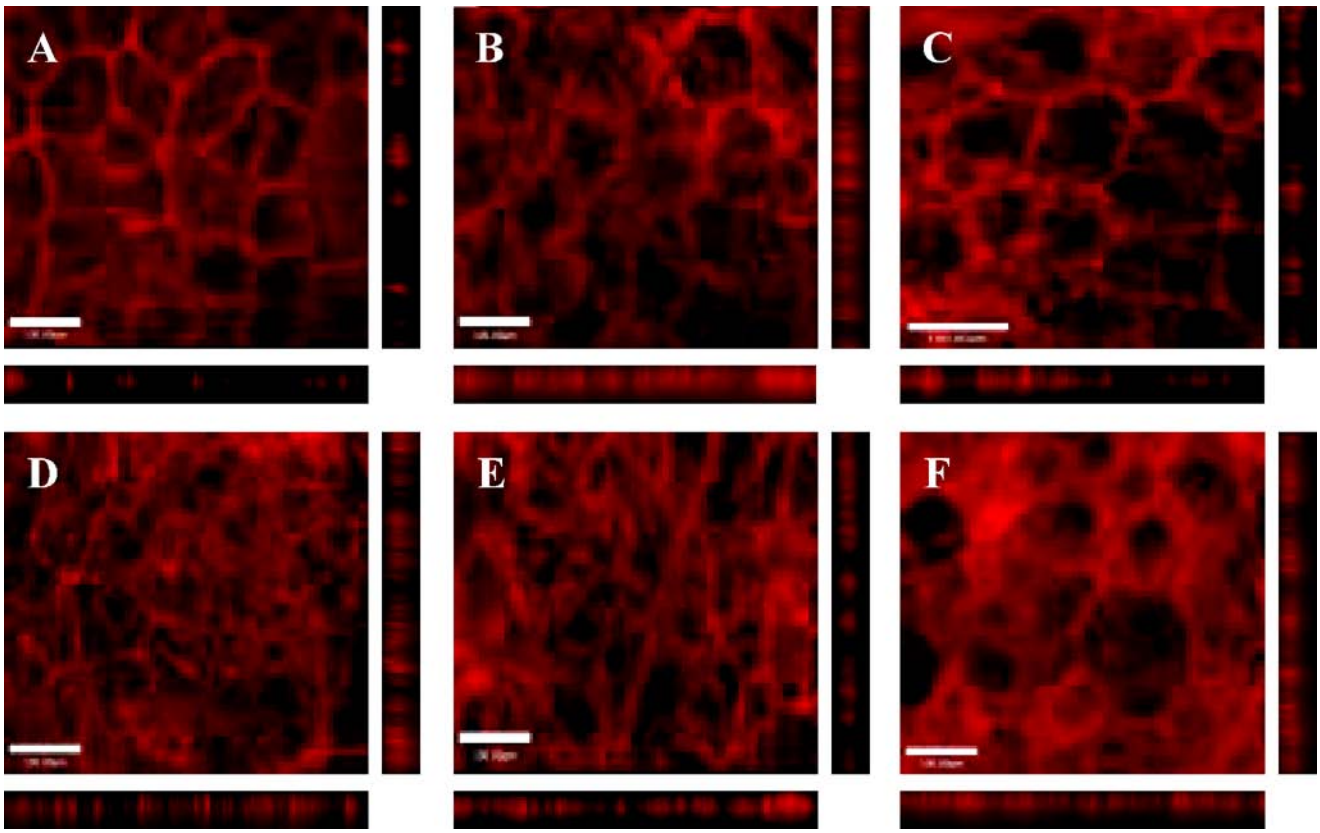

Fig. 5. Staining of the tight junction protein actin. (A) Caco-2 cells with no polymer treatment. Caco-2 cells incubated for 120 min with 1.0 mM: (B) $G2NH_2$; (C) G2OH, (D) G1.5COOH; (E) G2.5COOH; (F) G3.5COOH. Main panels illustrate the *xy* plane; horizontal bars illustrate the *xz* plane; vertical bars illustrate the *yz* plane. Scale bars equal 100.00 μm.

The increase in fluorescent signal compared to control cells was 34.2 ± 13.4%, 14.4 ± 4.0%, 50.8 ± 8.6%, 56.6 ± 5.9%, and 51.9 ± 7.5% (mean ± standard deviation, $n = 3$) for cells treated with $G2NH_2$, G2OH, G1.5COOH, G2.5COOH, and G3.5COOH, respectively. All dendrimers caused a significant increase in fluorescent signal compared to control cells ($P < 0.05$).

A similar, uniform staining pattern was observed for control cells treated with rhodamine phalloidin to visualize actin protein (Fig. 5A). Upon incubation with PAMAM dendrimers of 1.0 mM for 2 h, the staining pattern of rhodamine phalloidin became disruptive, and a significant increase in fluorescent signal ($P < 0.05$), except in the case of cells treated with G2OH, was observed within cell borders (Fig. 5B–F). Cells treated with $G2NH_2$, G2OH, G1.5COOH, G2.5COOH, and G3.5COOH dendrimers increased the fluorescent signal compared to control cells by 36.1 ± 3.5%, 13.1 ± 6.8%, 54.8 ± 20.9%, 44.6 ± 2.0%, and 63.3 ± 2.2% (mean ± standard deviation, $n = 3$), respectively. This is an indication that the structure of the actin filaments are compromised, thus resulting in condensation of actin within the cells. These observations are in agreement with the results from TEER measurements and ^{14}C-mannitol permeability: cells treated with cationic and anionic dendrimers had greater accumulation of occludin and actin proteins within the cell periphery, caused the greatest decline in TEER and enhanced ^{14}C-mannitol permeability. These results suggest PAMAM dendrimers modulate opening of tight junctions.

DISCUSSION

We have previously demonstrated that the dendrimers investigated in the current study are non-toxic at donor concentrations of 1.0 mM and up to 120 min incubation time (7,8). Here, we determined cell viability using the WST-1 toxicity assay that measures metabolic activity of Caco-2 cells. We observed that G3.5COOH dendrimers had greater permeability compared to the smaller dendrimers G1.5–G2.5COOH, $G2NH_2$ and G2OH (Fig. 1) without reducing cell viability (Table II). This is consistent with previous data by Duncan and coworkers in an everted sac model (5), and is a result of the greater anionic surface charge density that presumably modulates tight junctions by calcium chelation (8,17). We previously demonstrated that epithelial permeability of cationic dendrimers decreases with size (7), whereas here it is reported anionic dendrimer permeability increases with their size. This data is encouraging in that increased permeability of larger dendrimers facilitates surface conjugation or enhanced drug loading within the dendritic box, thereby enabling the utilization of these constructs for oral delivery of poorly bioavailable drugs. PAMAM dendrimers reduced cell monolayer electrical resistance after 2 h incubation with Caco-2 cells. Since all FITC-conjugated dendrimers (except $G2NH_2$) had a reversible effect on Caco-2 TEER (Fig. 2), this suggests their safe usage as oral drug delivery carriers.

To determine the influence of dendrimer surface charge on epithelial permeability, we investigated the transport of comparably sized PAMAM dendrimers while monitoring the ^{14}C-mannitol flux. The rank order of dendrimer permeability, as well as their concomitant reduction in TEER, was $G2NH_2$ > G1.5COOH > G2OH (Fig. 1). The charged dendrimers had greater permeability than G2OH, which has no net surface charge at physiological pH to enable its interaction with cell monolayers. Our previous studies suggest that cationic dendrimers are transported by a combination of paracellular and endocytic mechanisms (18). Hence, a combination of factors such as size and transport routes may explain, at least in part, the observed transport differences between small dendrimers.

^{14}C-Mannitol permeability was not affected by either FITC-labeled or native G2OH. However, the ^{14}C-mannitol flux significantly increased in the presence of FITC-labeled $G2NH_2$ and G1.5COOH dendrimers relative to their unlabeled counterparts (Fig. 3). To assess whether changes in cell permeability were due to intrinsic toxicity of the FITC label itself, we determined Caco-2 cell viability in the presence of increasing FITC concentrations using the WST-1 cytotoxicity assay. No significant effect was observed up to 1.0 mM FITC, which was the highest concentration conjugated to PAMAM dendrimers used in this study (Table I). Thus, the conjugation of FITC to charged dendrimers modifies their absorption enhancing effects, likely due to a change in physicochemical surface characteristics. This is an encouraging finding in that the conjugation of drug molecules to dendrimers may influence the extent to which the carriers are transported across the epithelial barrier of the gut.

In addition to altering permeability characteristics, it has been shown that surface modification of PAMAM dendrimers reduces their toxicity (10,11). Therefore, we investigated the effect on cell viability of a series of fluorescently labeled dendrimers with an incremental increase in the amount of conjugated FITC. As expected, at feed molar ratios of 1:1, 1:4, and 1:8 ($G4NH_2$:FITC) the toxicity of $G4NH_2$ dendrimers reduced with an increase in FITC label (Table I). Interestingly, $G4NH_2$-FITC (1:8) displayed the highest relative permeability (Fig. 1) with a concomitant increase in mannitol flux (Fig. 3), most likely due to a higher degree of tight junctional modulation. Although reduced cell viability cannot be excluded as a contributing factor to the increased permeability (Table II), it should be noted that monolayer integrity after exposure to these conjugates was reversible (Fig. 2). These data demonstrate that attachment of several hydrophobic drug molecules may result in appreciable permeability while the polymer-drug conjugate remains non-toxic to the epithelial barrier.

The ^{14}C-mannitol permeability and TEER data suggest a direct interaction between PAMAM dendrimers and cellular tight junctions (7,8,18). To confirm this hypothesis, we employed immunofluorescence microscopy to study changes in the barrier function of tight junctions. Tight junctions are protein complexes that include occludin, claudin, junctional-associated membrane protein (JAM), and zonula occludens proteins (ZO-1, ZO-2) (16, 19–21). Occludin protein is responsible for the fusion of adjacent plasma membranes to form the junction, which functions to maintain cellular integrity, along with Ca^{2+} and Mg^{2+} ions (22). A clear band of occludin protein was observed for untreated Caco-2 cells (Fig. 4A), whereas PAMAM dendrimer exposure resulted in increased accumulation of occludin protein as evidenced by the disruptive staining pattern encircling Caco-2 cells. This pattern indicates the opening of the tight junctions upon incubation with PAMAM dendrimers. Cells treated with cationic (Fig. 4B)

and anionic (Fig. 4D–F) dendrimers appear to have more disruptive staining pattern and greater accumulation of occludin than cells treated with neutral dendrimers (Fig. 4C). These data directly confirm that PAMAM dendrimers contribute to the opening of tight junctions.

Actin filaments are responsible for binding adjacent cells, thereby forming a single unit (22). Incubation of Caco-2 cell monolayers with rhodamine phalloidin, a specific probe for filamentous actin, revealed a clear, continuous staining pattern (Fig. 5A). Upon incubation with PAMAM dendrimers, however, the cells show a clear disruption of actin staining (Fig. 5B–F). These data correspond with the observations that cationic and anionic dendrimers cause a decline in TEER and enhance ^{14}C-mannitol permeability.

The studies reported here point to several phenomena that can be useful in the design of oral drug delivery systems based on poly(amidoamine) dendrimers. Higher generation anionic dendrimers can be suitable candidates because of their increased transport rate and low toxicity. The physicochemical characteristics of the conjugated molecules and the extent of conjugation can influence cell viability and permeability, and indeed tight junctional opening is, at least in part, responsible for the observed increase in the transport of dendrimers as well as paracellular markers such as ^{14}C-mannitol. The next logical steps are to investigate the endocytic behavior of dendrimers, the manner and extent by which they influence cell membranes, and design and develop novel systems by which these carriers can be beneficial in the oral delivery of biomolecules.

CONCLUSIONS

PAMAM dendrimer permeability is dependent on structural properties including size and surface charge. In the series studied, anionic dendrimer G3.5COOH and cationic G4NH$_2$ modified with 8 FITC molecules in the feed ratio showed the highest transport rates. Increase in the attachment of hydrophobic FITC label increased the permeability and reduced toxicity of G4NH$_2$. Finally, permeability and confocal microscopy studies suggest PAMAM dendrimers cause modulation of the tight junctions. The reported data demonstrates that by controlling size, surface charge and surface functionality it is possible to design dendrimers for optimized oral drug delivery applications.

ACKNOWLEDGMENTS

The authors would like to acknowledge Amy Foraker for her assistance with the confocal microscopy studies. Kelly Kitchens received financial support for this research by a predoctoral National Research Service Award from the National Institute of General Medical Sciences (F31-GM67278).

REFERENCES

1. N. Pantzar, L. Lundin, L. Wester, and B. R. Westrom. Bidirectional small-intestinal permeability in the rat to some common marker molecules. *Scand. J. Gastroenterol.* **29**:703–709 (1991).
2. D. A. Tomalia, A. M. Naylor, and W. A. Goddard III. Starburst dendrimers. Molecular-level control of size, shape, surface chemistry, topology, and flexibility from atoms to macroscopic matter. *Angew. Chem. Int. Ed. Engl.* **29**:138–175 (1990).
3. T. Kuhl, Y. Guo, J. L. Alderfer, A. D. Berman, D. Leckband, J. Israelachvili, and S. W. Hui. Direct measurement of polyethlyene glycol induced depletion attraction between lipid bilayers. *Langmuir* **12**:3003–3014 (1996).
4. R. Jevprasesphant, J. Penny, D. Attwood, and A. D'Emanuele. Transport of dendrimer nanocarriers through epithelial cells via the transcellular route. *J. Control. Release* **97**:259–267 (2004).
5. R. Wiwattanapatapee, B. Carreno-Gomez, N. Malik, and R. Duncan. Anionic. PAMAM dendrimers rapidly cross adult rat intestine *in vitro*: a potential oral delivery system? *Pharm. Res.* **17**:991–998 (2000).
6. F.Tajarobi, M. El-Sayed, B. D. Rege, J. E. Polli, and H. Ghandehari. Transport of poly amidoamine dendrimers across Madin-Darby Canine Kidney cells. *Int. J. Pharm.* **215**:263–267 (2001).
7. M. El-Sayed, M. Ginski, C. Rhodes, and H. Ghandehari. Transepithelial transport of poly(amidoamine) dendrimers across Caco-2 cell monolayers. *J. Control. Release* **81**:355–365 (2002).
8. M. El-Sayed, M. Ginski, C. Rhodes, and H. Ghandehari. Influence of surface chemistry of poly(amidoamine) dendrimers on Caco-2 cell monolayers. *J. Bioact. Compat. Polym.* **18**:7–22 (2003).
9. A. D'Emanuele, R. Jevprasesphant, J. Penny, and D. Attwood. The use of a dendrimer-propranolol prodrug to bypass efflux transporters and enhance oral bioavailability. *J. Control. Release* **95**:447–453 (2004).
10. R. Jevprasesphant, J. Penny, D. Attwood, N. B. McKeown, and A. D'Emanuele. Engineering of dendrimer surfaces to enhance transepithelial transport and reduce cytotoxicity. *Pharm. Res.* **20**:1543–1550 (2003).
11. R. Jevprasesphant, J. Penny, R. Jalal, D. Attwood, N. B. McKeown, and A. D'Emanuele. The influence of surface modification on the cytotoxicity of PAMAM dendrimers. *Int. J. Pharm.* **252**:263–266 (2003).
12. D. A. Tomalia. Birth of a new macromolecular architecture: dendrimers as quantized building blocks for nanoscale synthetic organic chemistry. *Aldrichimica Acta* **37**:39–57 (2004).
13. R. Esfand and D. A. Tomalia. Poly(amidoamine) (PAMAM) dendrimers: from biomimicry to drug delivery and biomedical applications. *Drug Discov. Today* **6**:427–436 (2001).
14. M. El-Sayed, M. F. Kiani, M. D. Naimark, A. H. Hikal, and H. Ghandehari. Extravasation of poly(amidoamine) (PAMAM) dendrimers across microvascular network endothelium. *Pharm. Res.* **18**:23–28 (2001).
15. J. D. Irvine, L. Takahashi, K. Lockhart, J. Cheong, J. W. Tolan, H. E. Selick, and J. R. Grove. MDCK (Madin-Darby Canine Kidney) cells: a tool for membrane permeability screening. *J. Pharm. Sci.* **88**:28–33 (1998).
16. F. A. Dorkoosh, C. A. Broekhuizen, G. Borchard, M. Rafiee-Tehrani, J. C. Verhoef, and H. E. Junginger. Transport of octreotide and evaluation of mechanism of opening the paracellular tight junctions using superporous hydrogel polymers in Caco-2 cell monolayers. *J. Pharm. Sci.* **93**:743–752 (2004).
17. A. B. J. Noach, Y. Kurosaki, M. C. M. Blom-Roosemalen, A. G. D. Boer, and D. D. Breimer. Cell-polarity dependant effect of chelation on the paracellular permeability of confluent Caco-2 cell monolayers. *Int. J. Pharm.* **90**:229–237 (1993).
18. M. El-Sayed, C. A. Rhodes, M. Ginski, and H. Ghandehari. Transport mechanism(s) of poly(amidoamine) dendrimers across Caco-2 cell monolayers. *Int. J. Pharm.* **265**:151–157 (2003).
19. Y. Chen, C. Merzdorf, D. L. Paul, and D. A. Goodenough. COOH terminus of occludin is required for tight junction barrier function in early Xenopus embryos. *J. Cell Biol.* **138**:891–899 (1997).
20. J. M. Anderson and C. M. van Itallie. Tight junctions and the molecular basis for regulation of paracellular permeability. *Am. J. Physiol.* **269**:G467–G475 (1995).
21. J. M. Anderson, C. M. van Itallie, M. D. Peterson, B. R. Stevenson, E. A. Carew, and M. S. Mooseker. ZO-1 mRNA and protein expression during tight junction assembly in Caco-2 cells. *J. Cell Biol.* **109**:1047–1056 (1989).
22. L. Knutson, F. Knutson, and T. Knutson. Permeability in the gastrointestinal tract. In J. B. D. H. Lennernäs (ed.), *Oral Drug Absorption: Prediction and Assessment*, Marcel Dekker, New York, 2000, pp. 11–16.